Poster ABCL-802

ARV-393, a PROTAC BCL6 Degrader, in Preclinical Models of Diffuse Large B-cell Lymphoma, Nodal T-Follicular Helper Cell Lymphoma, and Transformed Follicular Lymphoma

Anna Van Acker, Lynn DeCarr, Sarah Eaton, Dan Sherman, Elizabeth Bortolon, Mark Bookbinder, Jennifer Pizzano, Wendy Wu, John Corradi, Morena Scopel, William Corwin, Ignacio Juncadella, Ram Lingamaneni, Stephanie Renzullo, Emma Rousseau, Jennifer Cantley, XiaoZhe (Janet) Wang, Ian Taylor, Sean Landrette, Sheryl M Gough

Arvinas Operations, Inc., New Haven, CT, USA

Objective

- To evaluate the preclinical antitumor activity of ARV-393, a PROteolysis TArgeting Chimera (PROTAC) B-cell lymphoma 6 (BCL6) degrader, as a single agent in models of nodal T-follicular helper cell lymphoma, angioimmunoblastic-type (nTFHL-AI) and transformed follicular lymphoma (tFL), and in combination with small-molecule inhibitors (SMIs) of potentially cooperative oncogenic drivers in diffuse large B-cell lymphoma (DLBCL) models

Key Findings

- ARV-393 significantly reduced tumor burden in peripheral blood, bone marrow, and spleen in a cyclophosphamide, hydroxydaunorubicin, vincristine sulfate, and prednisone (CHOP)-relapsed nTFHL-AI patient-derived xenograft (PDX) model
- ARV-393 monotherapy resulted in robust (≥95%) tumor growth inhibition (TGI) in 2 tFL PDX models
- Changes at the transcriptional level detected by RNA sequencing in DLBCL cell lines suggest ARV-393 drives inhibition of cell cycle progression by decreasing early region 2 binding factor (E2F) pathway activity and promotes differentiation by increasing interferon (IFN) pathway activity
- ARV-393 demonstrated increased TGI in combination with all evaluated SMIs compared with the respective monotherapy treatments, with tumor regressions observed when ARV-393 was combined with tazemetostat, palbociclib, acalabrutinib, or venetoclax

Conclusions

- ARV-393 monotherapy demonstrated pronounced single-agent activity in a CHOP-relapsed PDX model of nTFHL-AI and in 2 PDX models of tFL, supporting clinical evaluation of ARV-393 in patients with these non-Hodgkin lymphoma (NHL) subtypes in addition to DLBCL
  - To our knowledge, this is the first preclinical evidence of an efficacious BCL6-targeted small-molecule degrader in human nTFHL-AI, an indication with a high unmet need
- Enhanced antitumor activity of ARV-393 in combination with 5 classes of SMIs together with mechanistic insights into the observed synergistic activity suggest that oral, chemotherapy-free approaches may warrant future clinical investigation in patients with DLBCL

Background

- The transcriptional repressor protein BCL6 is a critical regulator of germinal center formation and a lineage-defining transcription factor of T-follicular helper cells[1-4]
- BCL6 controls important cellular processes, including DNA damage repair, cell cycle progression, terminal differentiation, and programmed cell death, and is an established oncogenic driver of DLBCL[1,2]
- BCL6 has also been implicated in tFL and nTFHL, including nTFHL-AI, formerly angioimmunoblastic T-cell lymphoma[5-8]
- ARV-393, a PROTAC BCL6 degrader, directly binds an E3 ubiquitin ligase and BCL6 to induce the ubiquitination of BCL6 and its subsequent proteasomal degradation[9]
- ARV-393 rapidly degraded BCL6 in DLBCL cell lines and induced tumor regressions in PDX models of different DLBCL subtypes[10]
- ARV-393 demonstrated broad combinability with standard of care (SOC) chemotherapy and SOC biologics in a preclinical model of triple-hit high-grade B-cell lymphoma (HGBCL)[11]
- ARV-393 is being evaluated in a phase 1 trial (NCT06393738) in patients with NHL[12]
- Here, we explore ARV-393 as a single agent in models of nTFHL-AI and tFL and in combination with SMIs targeting major lymphoma-driving pathways in DLBCL models

Please scan the QR code to view **previously presented ARV-393 preclinical data.**[10] EHA 2024

Methods

ARV-393 monotherapy in nTFHL-AI and tFL models

- ARV-393 antitumor activity was assessed in a systemic PDX model developed from the tumor of a patient with nTFHL-AI who relapsed after CHOP therapy
  - ARV-393 30 mg/kg or vehicle was administered orally (PO) once daily (QD); romidepsin (histone deacetylase inhibitor) 1 mg/kg was administered intraperitoneally every 3 days
  - Tumor burden was measured via flow cytometry (human cluster of differentiation 2 [hCD2] and hCD45) and spleen weight
  - Tumor cell BCL6 protein levels in the spleen were evaluated via quantitative immunofluorescence (QIF)
- ARV-393 antitumor activity was assessed in 2 subcutaneous PDX models of tFL, LY9603 and LY9605
  - ARV-393 30 mg/kg or vehicle was administered PO QD

RNA sequencing analysis in DLBCL cell lines

- Transcriptional changes (relative to control) were evaluated 72 hours after ARV-393 treatment in 3 DLBCL cell lines: WSU-DLCL2 (HGBCL), OCI-Ly7 (germinal center B-cell [GCB]), and OCI-Ly10 (activated B-cell [ABC])

ARV-393 in combination with SMIs in DLBCL models

- ARV-393 was evaluated in combination with SMIs of enhancer of zeste homolog 2 (EZH2; tazemetostat), cyclin-dependent kinase 4/6 (CDK4/6; palbociclib), mammalian target of rapamycin (mTOR; everolimus), Bruton tyrosine kinase (BTK; acalabrutinib), and B-cell lymphoma 2 (BCL2; venetoclax) in subcutaneous cell line–derived xenograft (CDX) models of DLBCL
  - ARV-393 30 mg/kg PO QD was administered alone or in combination with tazemetostat, palbociclib, everolimus, or acalabrutinib; ARV-393 3 mg/kg PO QD was administered alone or in combination with venetoclax
  - Tazemetostat 300 mg/kg PO twice daily (BID), palbociclib 45 mg/kg PO QD, or everolimus 2 mg/kg PO QD was administered to mice bearing the *EZH2*-mutant SU-DHL-6 HGBCL CDX, acalabrutinib 2 mg/kg PO BID to mice bearing the *MYD88*-mutant OCI-Ly10 ABC DLBCL CDX, and venetoclax 100 mg/kg PO QD to mice bearing the *BCL2*-positive OCI-Ly1 GCB DLBCL CDX
  - One group of mice from each model received the vehicle PO QD

Results

ARV-393 Monotherapy in nTFHL-AI and tFL Models

- In the nTFHL-AI PDX model, ARV-393 demonstrated significant single-agent activity, reducing tumor burden in peripheral blood (8-fold decrease in hCD2+/hCD45+ cells, $P<0.01$), bone marrow (5-fold decrease in hCD2+/hCD45+ cells, $P<0.0001$), and spleen (3-fold decrease in weight, $P<0.001$; **Figure 1**)
  - ARV-393 performed similarly to romidepsin, a histone deacetylase inhibitor commonly used to treat patients with nTFHL-AI
  - Target engagement was confirmed by a reduction in BCL6 protein positivity in tumor cells as measured by QIF at study end
- In the 2 tFL PDX models, ARV-393 resulted in 95% and 99% TGI (**Figure 2**)
  - Target engagement was confirmed by a >99% reduction in BCL6 protein in tumor cell lysates at day 28

RNA Sequencing in DLBCL Cell Lines

- RNA sequencing revealed enrichment of E2F targets in genes significantly downregulated by ARV-393 (in WSU-DLCL2 and OCI-Ly7 cell lines), and enrichment of IFN response signaling in genes significantly upregulated by ARV-393 (in all 3 cell lines; **Figure 3**)
  - These data suggest that ARV-393–mediated degradation of BCL6 inhibits tumor cell cycle progression (by decreasing E2F pathway activity) and promotes differentiation (by increasing IFN pathway activity), a mechanism that may allow for broad combinability with inhibitors of other major lymphoma-driving pathways

ARV-393 in Combination With SMIs in DLBCL Models

- ARV-393 in combination with tazemetostat, palbociclib, or everolimus increased TGI compared to the respective monotherapy treatments, with tumor regressions (TGI ≥100%) observed with the tazemetostat and palbociclib combinations in the SU-DHL-6 HGBCL CDX model (**Figure 4A–C**)
  - EZH2, BCL2, and MYC protein levels increased by 66%,12%, and 56%, respectively, with ARV-393 alone vs vehicle, but decreased by 80%, 96%, and 75%, respectively, with ARV-393 plus tazemetostat vs vehicle, demonstrating a synergistic reduction in proteins known to drive lymphoma cell growth (**Figure 4A**)
- Marked tumor regressions were observed with ARV-393 in combination with acalabrutinib in the OCI-Ly10 ABC DLBCL CDX model (**Figure 4D**)
  - BCL6 upregulation was observed with single-agent acalabrutinib ($P<0.0001$), suggesting that BCL6 may play a role in resistance to this agent and providing a rationale for the observed synergy with ARV-393
- Complete tumor regressions were observed with ARV-393 in combination with venetoclax in the OCI-Ly1 GCB DLBCL CDX model (**Figure 4E**)

Figure 1: Single-agent ARV-393 antitumor effect in a PDX model of relapsed nTFHL-AI

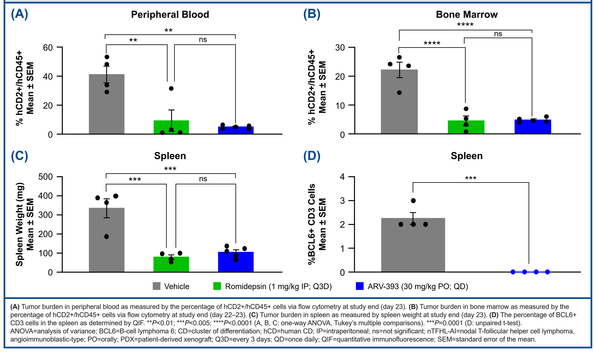

(A) Tumor burden in peripheral blood as measured by the percentage of hCD2+/hCD45+ cells via flow cytometry at study end (day 23). **(B)** Tumor burden in bone marrow as measured by the percentage of hCD2+/hCD45+ cells via flow cytometry at study end (day 22–23). **(C)** Tumor burden in spleen as measured by spleen weight at study end (day 23). **(D)** The percentage of BCL6+ CD3 cells in the spleen as determined by QIF. **$P<0.01$; ***$P<0.005$; ****$P<0.0001$ (A, B, C: one-way ANOVA, Tukey's multiple comparisons); ***$P<0.0001$ (D: unpaired t-test).
ANOVA=analysis of variance; BCL6=B-cell lymphoma 6; CD=cluster of differentiation; hCD=human CD; IP=intraperitoneal; ns=not significant; nTFHL-AI=nodal T-follicular helper cell lymphoma, angioimmunoblastic-type; PO=orally; PDX=patient-derived xenograft; QD=every 3 days; QD=once daily; QIF=quantitative immunofluorescence; SEM=standard error of the mean.

Figure 2: Single-agent ARV-393 antitumor effect in PDX models of tFL

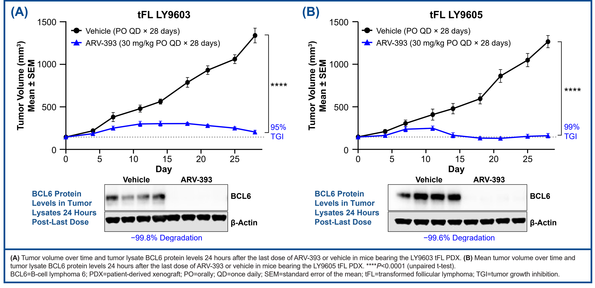

(A) Tumor volume over time and tumor lysate BCL6 protein levels 24 hours after the last dose of ARV-393 or vehicle in mice bearing the LY9603 tFL PDX. **(B)** Mean tumor volume over time and tumor lysate BCL6 protein levels 24 hours after the last dose of ARV-393 or vehicle in mice bearing the LY9605 tFL PDX. ****$P<0.0001$ (unpaired t-test).
BCL6=B-cell lymphoma 6; PDX=patient-derived xenograft; PO=orally; QD=once daily; SEM=standard error of the mean; tFL=transformed follicular lymphoma; TGI=tumor growth inhibition.

Figure 3: ARV-393 effect on E2F target and IFN response genes across DLBCL cell lines

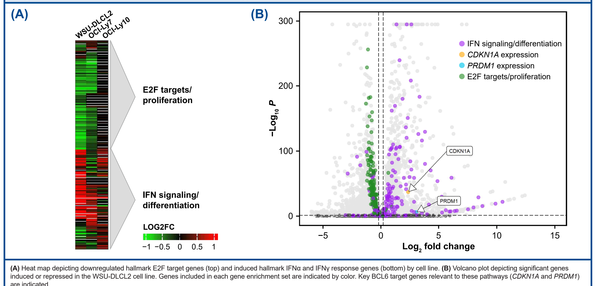

(A) Heat map depicting downregulated hallmark E2F target genes (top) and induced hallmark IFNα and IFNγ response genes (bottom) by cell line. **(B)** Volcano plot depicting significant genes induced or repressed in the WSU-DLCL2 cell line. Genes included in each gene enrichment set are indicated by color. Key BCL6 target genes relevant to these pathways (*CDKN1A* and *PRDM1*) are indicated.
BCL6=B-cell lymphoma 6; *CDKN1A*=cyclin-dependent kinase inhibitor 1A gene; DLBCL=diffuse large B-cell lymphoma; E2F=early region 2 binding factor; IFN=interferon; LOG2FC=log2 fold change; *PRDM1*=PR domain zinc finger protein 1 gene.

Figure 4: ARV-393 antitumor effect in combination with SMIs

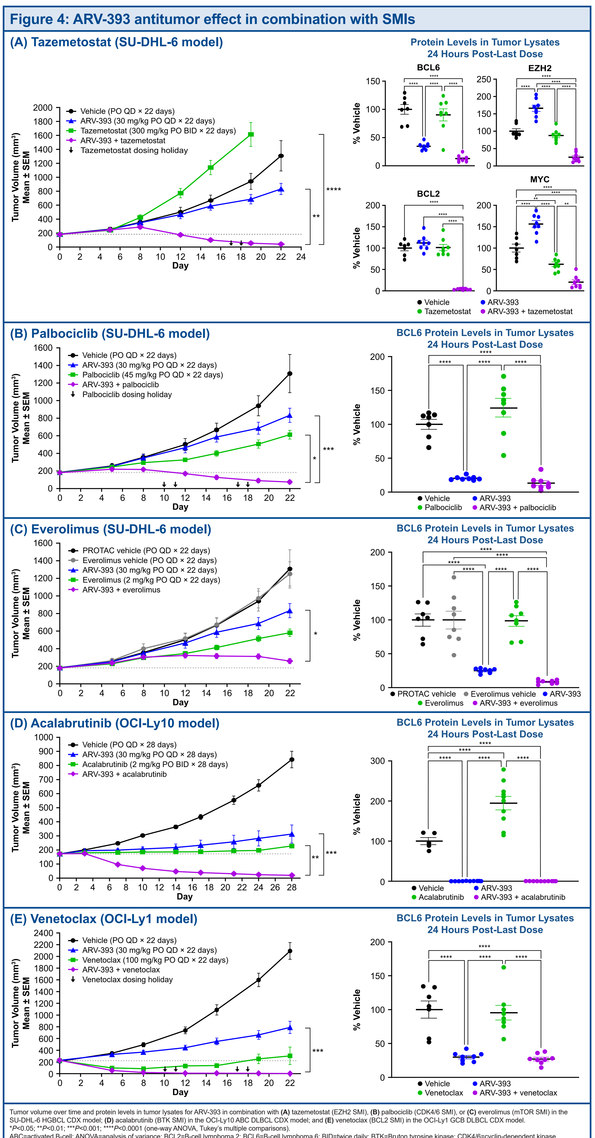

Tumor volume over time and protein levels in tumor lysates for ARV-393 in combination with **(A)** tazemetostat (EZH2 SMI), **(B)** palbociclib (CDK4/6 SMI), or **(C)** everolimus (mTOR SMI) in the SU-DHL-6 HGBCL CDX model; **(D)** acalabrutinib (BTK SMI) in the OCI-Ly10 ABC DLBCL CDX model; and **(E)** venetoclax (BCL2 SMI) in the OCI-Ly1 GCB DLBCL CDX model.
*P<0.05; **P<0.01; ***P<0.001; ****P<0.0001 (one-way ANOVA, Tukey's multiple comparisons).
ABC=activated B-cell; ANOVA=analysis of variance; BCL2=B-cell lymphoma 2; BCL6=B-cell lymphoma 6; BID=twice daily; BTK=Bruton tyrosine kinase; CDK4/6=cyclin-dependent kinase 4/6; CDX=cell line–derived xenograft; DLBCL=diffuse large B-cell lymphoma; EZH2=enhancer of zeste homolog 2; GCB=germinal center B-cell; HGBCL=high-grade B-cell lymphoma; mTOR=mammalian target of rapamycin; PO=orally; QD=once daily; SEM=standard error of the mean; SMI=small-molecule inhibitor.

References

1. Basso K and Dalla-Favera R. *Immunol Rev*. 2012;247(1):172-83.
2. Hatzi K and Melnick A. *Trends Mol Med*. 2014;20(6):343-52.
3. Choi J, et al. *Nat Immunol*. 2020;21(7):777-89.
4. Nurieva RI, et al. *Science*. 2009;325(5943):1001–5
5. Szeredy Z, et al. *Am J Pathol*. 2000;156(3):1017-24.
6. Aksaka T, et al. *Blood*. 2003;102(4):1443-8.
7. Nishizawa S, et al. *Int J Hematol*. 2017;105(4):465-9.
8. Witalis M, et al. *Blood Adv*. 2020;4(5):868-79.
9. Sherman D, et al. Presented at AACR; April 5–10, 2024; San Diego, CA, USA. Abstract ND-05.
10. Gough S, et al. Poster presented at EHA; June 13–16, 2024; Madrid, Spain. Poster P1256.
11. Van Acker A, et al. Poster presented at AACR; April 25–30, 2025; Chicago, IL, USA. Poster 1655.
12. Caimi PF, et al. Poster presented at AACR Advances in Malignant Lymphoma; June 19–22, 2024; Philadelphia, PA, USA. Poster PO-010.
13. Wright GW, et al. *Cancer Cell*. 2020;37(4):551-68.e14.

Acknowledgments

This research was funded by Arvinas, Inc. Medical writing support was provided by Charlotte Pettigrew, PhD, of Red Nucleus and was funded by Arvinas Operations, Inc.

Contacts

Anna Van Acker; anna.chiarella@arvinas.com
Sheryl Gough; sheryl.gough@arvinas.com

Data were previously presented at the European Hematology Association (EHA) Annual Congress; Milan, Italy; June 12–15, 2025

Society of Hematologic Oncology (SOHO) Annual Meeting; Houston, TX, USA; September 3–6, 2025